EBioMedicine 6 (2016) 50–58

Contents lists available at ScienceDirect

EBioMedicine

journal homepage: www.ebiomedicine.com

Research Paper

Targeting myeloid-derived suppressor cells with colony stimulating factor-1 receptor blockade can reverse immune resistance to immunotherapy in indoleamine 2,3-dioxygenase-expressing tumors

Rikke B. Holmgaard [a], Dmitriy Zamarin [a,b,c,d], Alexander Lesokhin [a,b,c,d], Taha Merghoub [a], Jedd D. Wolchok [a,b,c,d,*]

[a] Swim Across America/Ludwig Collaborative Laboratory, Memorial Sloan Kettering Cancer Center, New York, NY, United States
[b] Department of Medicine, Memorial Sloan-Kettering Cancer Center, New York, NY, United States
[c] Weill Cornell Medical College, New York, NY 10065, United States
[d] Graduate School of Medical Sciences of Cornell University, New York, NY 10065, United States

ARTICLE INFO

Article history:
Received 27 November 2015
Received in revised form 11 February 2016
Accepted 12 February 2016
Available online 13 February 2016

Keywords:
Immunotherapy
IDO
MDSCs
CSF-1R
CTLA-4
PD-1

ABSTRACT

Tumor indoleamine 2,3-dioxygenase (IDO) promotes immunosuppression by direct action on effector T cells and Tregs and through recruitment, expansion and activation of myeloid-derived suppressor cells (MDSCs). Targeting of MDSCs is clinically being explored as a therapeutic strategy, though optimal targeting strategies and biomarkers predictive of response are presently unknown. Maturation and tumor recruitment of MDSCs are dependent on signaling through the receptor tyrosine kinase CSF-1R on myeloid cells. Here, we show that MDSCs are the critical cell population in IDO-expressing B16 tumors in mediating accelerated tumor outgrowth and resistance to immunotherapy. Using a clinically relevant drug, we show that inhibition of CSF-1R signaling can functionally block tumor-infiltrating MDSCs and enhance anti-tumor T cell responses. Furthermore, inhibition of CSF-1R sensitizes IDO-expressing tumors to immunotherapy with T cell checkpoint blockade, and combination of CSF-1R blockade with IDO inhibitors potently elicits tumor regression. These findings provide evidence for a critical and functional role for MDSCs on the *in vivo* outcome of IDO-expressing tumors.

1. Introduction

Recent developments in cancer immunotherapies have demonstrated durable responses, suggesting that effective immunotherapy would hold promise to improve patient outcome (Gunturu et al., 2013; Hodi et al., 2003; Lutz et al., 2011; Ribas et al., 2009). However, attempts to use immunotherapeutics as single agents have achieved only limited clinical success (Hodi et al., 2010; Le et al., 2013; Phan et al., 2003; Robert et al., 2011; Royal et al., 2010). The resistance to immunotherapy is in part mediated by the immunosuppressive microenvironment in the tumor tissue, and identification of such mechanisms is highly prudent in order to develop appropriate combination strategies. Multiple suppressive mechanisms have been implicated in the resistance to checkpoint blockade, including accumulation of myeloid-derived suppressor cells (MDSCs) and increased expression of indoleamine 2,3-dioxygenase (IDO).

MDSCs use several mechanisms to induce immunosuppression, such as production of arginase I (Arg1) and inducible nitric oxide synthase (iNOS), leading to T-cell inhibition (Gabrilovich and Nagaraj, 2009). MDSCs can also promote tumor cell proliferation, confer resistance to cytotoxic therapies, and facilitate metastatic dissemination and angiogenesis (Gabrilovich and Nagaraj, 2009). Therefore, high numbers of tumor-infiltrating MDSCs are often associated with high tumor burden and metastatic disease, leading to poor survival in cancer patients (Diaz-Montero et al., 2009). Therapeutic targeting of MDSCs might overcome immunosuppression to enhance responses to immunotherapy.

Targeting of the colony stimulating factor-1 receptor (CSF-1R) has emerged as a strategy to ablate MDSCs or inhibit their tumor-promoting functions (Manthey et al., 2009; Patel and Player, 2009). CSF-1 is a cytokine frequently produced by several cancers, including melanoma, pancreatic cancer, and breast cancer (Priceman et al., 2010; Richardsen et al., 2015; Tarhini et al., 2012; Zhu et al., 2014). Secreted CSF-1 binds to the tyrosine kinase receptor CSF-1R on myeloid cells, which results in increased proliferation and differentiation of myeloid cells into MDSCs and M2 macrophages, and their recruitment into tumors (Caescu et al., 2015; Dai et al., 2002).

* Corresponding author at: Memorial Sloan Kettering Cancer Center, 1275 York Avenue, Box 470, New York, NY 10065, United States.
E-mail address: wolchokj@mskcc.org (J.D. Wolchok).

http://dx.doi.org/10.1016/j.ebiom.2016.02.024

Therefore, an immunosuppressive tumor microenvironment mediated by CSF-1 may limit the anti-tumor activity of tumor immunotherapy and lead to low response rates (Kerkar and Restifo, 2012). PLX647 is an analog of PLX3397, which is a potent CSF-1R inhibitor currently in clinical development as a single agent and in combination for the treatment of cancer patients. Recent work in preclinical models shows that CSF-1R inhibition inhibits the immunosuppressive tumor microenvironment and facilitates immune responses to cancer (Aharinejad et al., 2004; Coniglio et al., 2012; DeNardo et al., 2011; Mok et al., 2014; Priceman et al., 2010; Xu et al., 2013).

Despite these findings, its relation with known suppressive mechanisms is unclear and what biomarkers would predict sensitivity to CSF-1R inhibition is not well defined. Here, we examine the possibility of circumventing IDO suppression by targeting MDSCs in IDO-expressing tumors. Indeed, while studying the role of IDO in the tumor microenvironment, we previously found that overexpression of IDO by tumor cells (B16-IDO) promotes the recruitment of large numbers of highly suppressive MDSCs (Holmgaard et al., 2015). We took advantage of this tumor model to examine the possibility of abolishing the suppressive effect of IDO by targeting MDSCs in IDO-expressing tumors. We studied the role of the MDSCs in mediating resistance to immunotherapies and to develop rationally designed combinatorial immunotherapeutic approaches through CSF-1R targeting. Our data demonstrate that CSF-1R blockade with PLX647 depletes suppressive MDSCs and delays tumor growth in the B16-IDO tumor model dominated by MDSCs, but not in the control B16 tumor model. Inhibition of CSF-1R signaling functionally blocks MDSCs and enhances anti-tumor T cell responses and therefore partially rescue immune suppression conferred by IDO expression. Thus, our data demonstrate a reversal of IDO induced immunosuppression by targeting MDSCs through CSF-1R blockade. Moreover, we demonstrate that targeting of CSF-1R sensitized the tumors to immunotherapy with Cytotoxic T Lymphocyte-Associated Protein-4 (CTLA-4), Programmed Cell Death Protein-1 (PD-1), or IDO blockade. Previous work suggests that IDO promotes immune suppression by direct action on effector T cells and/or regulatory T cells (Tregs). Our findings suggest that both T cells and MDSCs contribute to IDO suppressive effects and as a result provide a strong rationale to reprogram immunosuppressive MDSCs in the tumor microenvironment under conditions that can significantly improve the effects of other immunotherapeutic agents that target T cells and IDO. Supporting these findings, we find that CSF-1R blockade also potentiates antitumor responses to T cell checkpoint immunotherapy in other animal tumor models. Importantly, this potentiation was only seen in tumors highly infiltrated with suppressive MDSCs, suggesting that the presence of MDSCs could serve as a pre-treatment biomarker that could predict the efficacy of such combination in patients.

2. Materials and Methods

2.1. Mice

C57BL/6J and Balb/c mice (6–8 weeks old) were purchased from Jackson Laboratory. Pmel-1 TCR transgenic mice have been reported (Overwijk et al., 2003) and were provided by N. Restifo (National Cancer Institute, Bethesda, MD). All mice were maintained in microisolator cages and treated in accordance with the NIH and American Association of Laboratory Animal Care regulations. All mouse procedures and experiments for this study were approved by the Memorial Sloan Kettering Cancer Center Institutional Animal Care and Use Committee.

2.2. Cell Lines

The murine cancer cell line for melanoma (B16F10, referred to as B16) and colon cancer (CT26) were maintained in RPMI medium supplemented with 10% fetal calf serum (FCS) and penicillin with streptomycin (complete RPMI media). The Flt3L-secreting B16 cell line was used to increase the number of APCs recruited to the spleen before purification of dendritic cells (DCs) (Curran and Allison, 2009).

2.3. Transduction of B16 Cells

B16-IDO was generated by transduction of B16F10 with *GFP* plus the *IDO* gene as previously described (Holmgaard et al., 2013). Briefly, GFP-tagged murine IDO cDNA (Origene Technologies) was cloned into the pMDG lentiviral vector. Recombinant virus production and infection of target cells were done as described (Diatta et al., 2005). B16F10 transduced with *GFP* alone were used as control cells (B16-WT).

2.4. Tumor Challenge and Treatment Experiments

On day 0 of the experiments, tumor cells were injected intradermally (i.d.) in the right flank. For the B16 model, 2.5×10^5 B16-WT or B16-IDO cells were injected into C57BL/6J mice and for the CT26 model, 5×10^5 CT26 cells were used in Balb/c mice. Treatments were given as single agents or in combinations with the following regimen for each drug. The IDO inhibitor drug indoximod/D-1MT (IDO*i*) was either dissolved in methylcellulose and administered in drinking water (2 mg/ml, mice drank 4.5–5.5 ml/day, Sigma-Aldrich) or formulated and administered in implantable subcutaneous pellets (140 mg/pellet, 14-day-release, Innovative Research of America). Treatment with IDO*i* was initiated on day 1 ending on day 15 post tumor challenge. Control groups received placebo pellets without the active product (Innovative Research of America). Anti-CTLA-4 antibody (100 μg/mouse, clone 9H10, Bio X cell) and anti-PD-1 antibody (250 μg/mouse, clone RPM1-14, Bio X cell) were injected intraperitoneally (i.p.) on days 3, 6 and 9 for the B16 model and on days 10, 13 and 16 for the CT26 model. Control groups received a corresponding dose of isotype antibody i.p. The CSF-1R kinase inhibitors, PLX647 and PLX5622 incorporated into rodent chow, were provided along with control chow by Plexxikon Inc. (800 ppm chow). Treatment with PLX647 or control chows was started at day 0 for the B16 model and on day 10 for the CT26 model, and continued for the remainder of the experiment. For *in vivo* T cell depletion experiments, mice were injected i.p. with 500 μg of monoclonal antibodies to CD8 (clone 2.43) or CD4 (clone GK1.5), 1 day before and 2 days after tumor challenge, followed by injection of 250 μg every 5 days throughout the experiment. The efficacy of cell depletion was verified by staining peripheral blood leukocytes for specific subsets after depletion. Tumors were measured every second or third day with a caliper, and the volume (length × width × height) was calculated. The animals were euthanized for signs of distress or when the total tumor volume reached 1000 mm^3.

2.5. Isolation of Tumor-infiltrating Cells and Lymphoid Tissue Cells

Mouse tumor samples were minced with scissors prior to incubation with 1.67 U/ml Liberase (Roche) and 0.2 mg/ml DNase (Roche) in RPMI for 30 min at 37 °C. Tumor samples were homogenized by repeated pipetting and filtered through a 100-μm nylon filter (BD Biosciences) in RPMI supplemented with 7.5% FCS to generate single-cell suspensions. Cell suspensions were washed once with complete RPMI and purified on a Ficoll gradient to eliminate dead cells. Cells from mouse spleens were isolated by grinding spleens through 100-μm filters. After red blood cell (RBC) lysis (ACK Lysing Buffer, Lonza) when required, all samples were washed and re-suspended in FACS buffer (PBS/2%FCS).

2.6. Flow Cytometry and Morphology Analysis

Cells isolated from mouse tumors and spleens were pre-incubated (15 min, 4 °C) with anti-CD16/32 monoclonal antibody (Fc block, clone 2.4G, BD Biosciences) to block nonspecific binding and then stained (30 min, 4 °C) with appropriate dilutions of various combinations of the

following fluorochrome-conjugated antibodies: anti-CD3-eFluor 450 (clone 17A2), anti-MHC Class II-eFluor 450 (clone M5/114.15.2), anti-CXCR3-PE (clone CXCR3-173), anti-CSF-1R-PE (clone AFS98), anti-CXCR3 (clone CXCR3-173), anti-CTLA-4-PE (clone UC10-4B9), anti-CD8-PE Texas Red (clone 5H10), anti-Gr1-PerCP-Cy5.5 (clone R86-8C5), anti-CD4-PE-Cy7 (clone RM4-5), anti-Granzyme B-PE-Cy7 (clone NGZB), anti-PD-1-PE-Cy7 (clone J43), anti-CD45-APC (clone 104), anti-F4/80-APC (clone BM8), anti-Foxp3-Alexa Fluor 700 (clone FJK-16S), anti-CD11c-Alexa Fluor 700 (clone N418), and anti-CD11b-APC eFluor 780 (clone M1/70) antibodies, all purchased from BD Biosciences, eBioscience or Invitrogen. The cells were further permeabilized using a FoxP3 Fixation and Permeabilization Kit (eBioscience) and stained for Foxp3 (clone FJK-16s, Alexa-Fluor-700-conjugated, eBioscience) and Ki67 (clone SolA15, eFluor-450-conjugated, eBioscience). The stained cells were acquired on a LSRII Flow Cytometer using BD FACSDiva software (BD Biosciences) and the data were processed using FlowJo software (Treestar). Dead cells and doublets were excluded on the basis of forward and side scatter.

2.7. DC Purification and Loading

Mice were injected subcutaneously with 2×10^6 Flt3L-secreting B16 cells and sacrificed after 2 weeks. Spleens were digested with 1.67 U/ml Liberase (Roche) and 0.2 mg/ml DNase (Roche) in RPMI for 30 min at 37 °C. Samples were filtered through a 100-μm nylon filter (BD Biosciences) and purified on a Ficoll gradient, before positive selection of CD11c + DCs according to the manufacturer's instructions (Miltenyi). DCs were cultured overnight with 10 ng/ml recombinant GM-CSF (PeproTech) and B16 tumor lysate in a 4:1 ratio of dead tumor cells to DCs. After loading, DCs were purified by Ficoll gradient (Sigma).

2.8. Tumor Lysate

Tumor cell lysate was prepared by radiation (140 Gy) followed by 5 rounds of freezing and thawing to lyse the tumor cells. Nuclear debris was removed by centrifugation. Cell lysate was filtered and cell death was verified using Trypan blue dye exclusion.

2.9. T Cell Assays

For cytokine production, tumor-infiltrating lymphocytes (TILs) were incubated overnight with DCs loaded with tumor lysate and 20 U/ml IL-2 (PeproTech). Brefeldin A (BD Biosciences) at 10 μg/ml was added for the last 4–5 h of stimulation. After *in vitro* stimulation, TILs were stained for intracellular cytokines with a FoxP3 Fixation and Permeabilization Kit (eBioscience) using antibody to anti-IFNγ-FITC (clone XMG1.2).

2.10. Purification of MDSCs

Mouse tumor and spleen single-cell suspensions were generated as described in the previous section. Tumor cells were subsequently separated from debris over a Ficoll gradient (Sigma-Aldrich). B cells were depleted from splenocytes using CD19 microbeads and LD columns according to the manufacturer's instructions (Miltenyi Biotec) to enrich the myeloid fractions. Cells were stained with anti-CD45.2-Alexa-Fluor-700, anti-CD11b-APC-Cy7 and anti-Gr1-PerCP-Cy5.5 antibodies for flow sorting on a FACSAria™ II Cell Sorter (BD Biosciences). Dead cells were excluded using DAPI (Invitrogen). Purity of flow-sorted populations was above 90%.

2.11. T cell Suppression Assay with MDSCs

Spleens and lymph nodes from naive mice were isolated and ground through 100-μm filters to generate a single cell suspension. After RBC lysis, $CD8^+$ cells were purified using anti-CD8 (Ly-2) microbeads (Miltenyi Biotech) according to manufacturer's protocol and labeled with 1 mM CFSE (Invitrogen) in pre-warmed PBS for 10 min at 37 °C. The CFSE-labeled $CD8^+$ T cells were then plated in complete RPMI media supplemented with 0.05 M β-mercaptoethanol onto round bottom 96-well plates (1×10^5 cells per well) coated with 1 μg/ml anti-CD3 (clone 1454-2C11) and 5 μg/ml anti-CD28 (clone 37N) antibodies. Purified MDSCs were added in indicated ratios and plates were incubated at 37 °C. After 48 h, cells were harvested and CFSE signal in the gated $CD8^+$ T cells was measured by flow cytometry (LSRII Flow Cytometer, BD Biosciences).

2.12. Isolation of Pmel Lymphocytes and Adoptive Transfer

Spleens and lymph nodes from pmel-1 TCR transgenic mice were isolated and ground through 100-μm filters. After RBC lysis, $CD8^+$ cells were purified by positive selection using Miltenyi magnetic beads. The isolated cells were loaded with CellTrace™ Far Red DDAO-SE (Thermo Fisher Scientific) and injected into recipient animals *via* tail vein at indicated numbers. Activated $CD8^+$ T cells were generated by culturing splenocytes with soluble anti-CD3 (1 μg/ml, clone 145-2C11, eBioscience) and anti-CD28 (2 μg/ml, clone 37.51, eBioscience) for 72 h. Recombinant mouse IL-2 (30 U/ml, Chiron) was added for the final 24 h of culture. $CD8^+$ T cells were subsequently positively selected with Miltenyi magnetic beads prior to injection *via* tail vein, as described above. The frequency and proliferation of pmel cells were measured 2 weeks after tumor challenge and 7 days after adoptive transfer of 1×10^6 *in vitro* activated $CD8^+$ pmel T cells using Thy1.1 antibody and by assessing CellTrace™ Far Red DDAO-SE dilution by flow cytometry, respectively.

2.13. Statistics

Where indicated, data were analyzed for statistical significance and reported as P values. Data were analyzed by 2-tailed Student's *t* test when comparing means of two independent groups and two-way ANOVA when comparing more than two groups. $P < 0.05$ was considered statistically significant ($^*P < 0.05$, $^{**}P < 0.01$, $^{***}P < 0.001$, $^{****}P < 0.0001$). Evaluation of survival patterns in tumor-bearing mice was performed by the Kaplan–Meier method, and results were ranked according to the Mantel–Cox log-rank test. $P < 0.05$ was considered statistically significant ($^*P < 0.05$, $^{**}P < 0.01$, $^{***}P < 0.001$, $^{****}P < 0.0001$). Survival was defined as mice with tumors $<1.000\ cm^3$.

3. Results

3.1. Expression of IDO by Tumors Results in Recruitment of CSF-1R Expressing MDSCs

As we have previously reported (Holmgaard et al., 2015), expression of IDO by tumor cells (B16-IDO) results in expansion of myeloid $CD11b^+$ cells in the tumor and spleen (Fig. 1a), which is dominated by an increase in frequencies of monocytic $CD11b^+Gr1^{int}$ cells (Fig. 1b). The $CD11b^+Gr1^{int}$ cells purified from B16-IDO tumors suppress CD8 T cell proliferation *in vitro*, consistent with their functional definition of MDSCs (Fig. 1c). Furthermore, these tumors were resistant to immunotherapy with CTLA-4 + PD-1 blockade, when compared to the wild type B16 tumors (B16-WT) (Fig. 1d). To determine whether the MDSCs were primary mediators of suppression and to develop appropriate strategies to block them, we focused on CSF-1R, which has been previously shown to play a role in MDSC development (Dai et al., 2002; Li et al., 2006). Phenotypic analysis of the Gr1 positive populations revealed that $CD11b^+Gr1^{int}$ cells, but not $CD11b^+Gr1^{high}$ cells, from tumors and spleens of B16-IDO tumor-bearing mice express high levels of CSF-1R (Fig. 1e). On the basis of these observations, we proceeded to determine the role of CSF-1R in our tumor model.

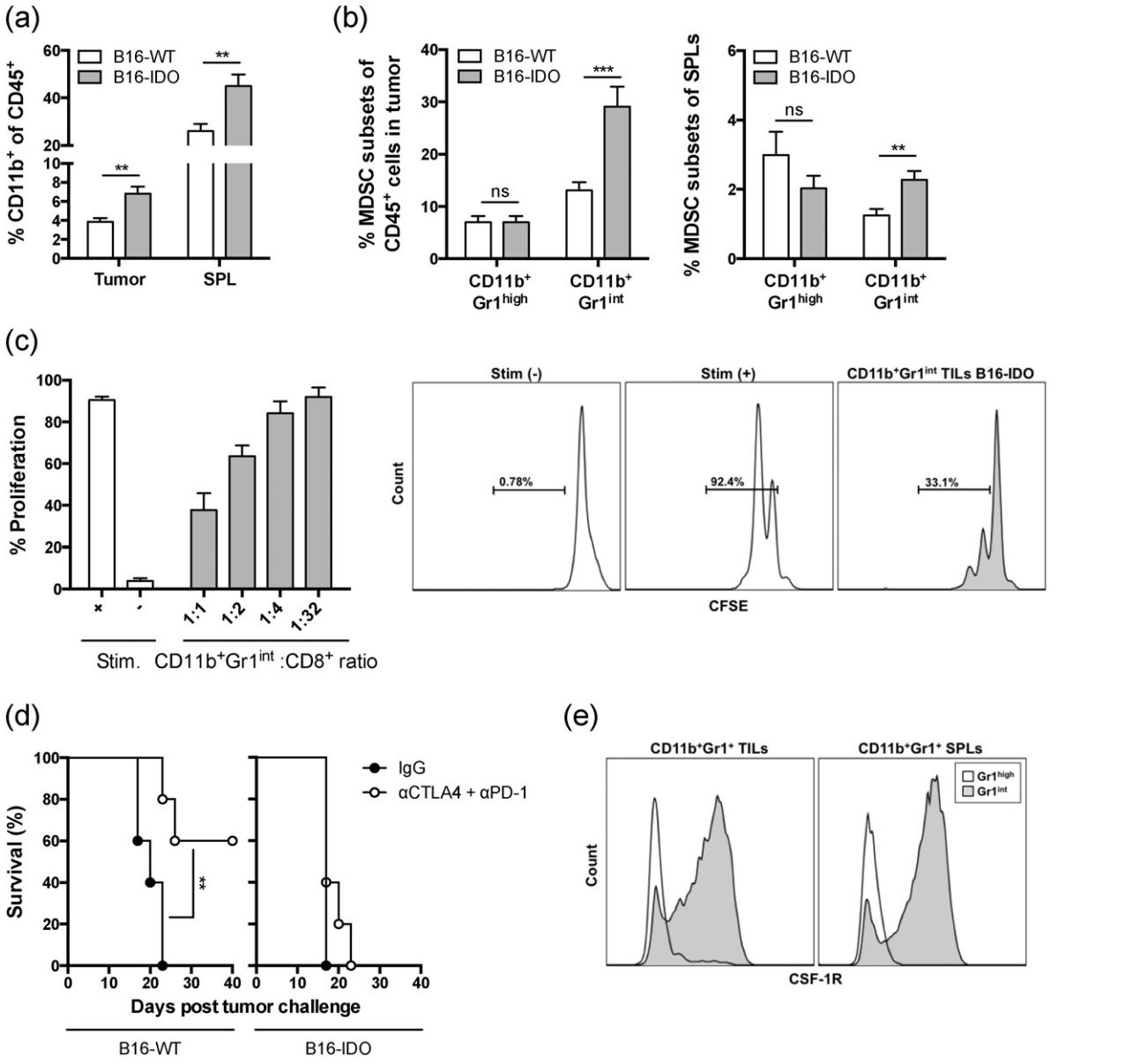

Fig. 1. IDO positive tumors show increased infiltration of CSF-1R expressing MDSCs. (a) B16-IDO and B16-WT tumors and spleens were harvested 2 weeks after tumor cell inoculation and analyzed for infiltration with MDSC subsets. Results are shown for total myeloid cells ($CD11b^+$) as frequencies of $CD45^+$ cells. (b) Frequencies of $CD11b^+Gr1^{high}$ and $CD11b^+Gr1^{int}$ subsets of total $CD45^+$ TILs and $CD45^+$ splenocytes. (c) *In vitro* suppressive activity of tumor-infiltrating $CD11b^+Gr1^{int}$ cells purified from B16-IDO tumor-bearing mice. Percent $CD8^+$ T cell proliferation (left panel) and representative histograms of $CD8^+$ T cell proliferation in $CD11b^+$ to $CD8^+$ T cell ratio of 1:1 (right panel). (d) Long-term survival of anti-CTLA-4 + PD-1 treated B16-IDO and B16-WT tumor-bearing mice. (e) Expression of CSF-1R in $Gr1^{int}$ and $Gr1^{high}$ cells within the $CD11b^+$ gated population of TILs and splenocytes of B16-IDO tumor-bearing mice. Data depicted are mean ± SEM from 3 independent experiments with 5–10 mice/group.

3.2. Blockade of CSF-1R Signaling Retards Tumor Growth of Tumors with High MDSC Infiltration by Depletion of Suppressive $CD11b^+Gr1^{int}$ MDSCs

Several compounds have been developed to specifically target CSF-1R. PLX647 is a small molecule receptor tyrosine kinase inhibitor inhibiting signaling from CSF-1R and KIT (Elmore et al., 2014; Zhang et al., 2013). To study the effects of PLX647 on B16-IDO tumors, mice were challenged with B16-IDO tumor cells and treated with PLX647 chow. In order to understand the impact of CSF-1R blockade on Gr1 subsets, we compared the composition of $Gr1^+$ cell populations from B16-IDO tumors following a 2-week treatment with either PLX647 or control chow. PLX647 treatment resulted in a significant reduction in the number of CSF-1R expressing $CD11b^+Gr1^{int}$ cells in the spleens, tumor-draining lymph nodes (TDLNs), and tumors of B16-IDO tumor-bearing mice (Fig. 2a), which was the population that we found to be suppressive in the functional assays (Fig. 1c). In contrast, the CSF-1R non-expressing granulocytic $CD11b^+Gr1^{high}$ population was not affected by PLX647 therapy (Fig. 2a). Consistent with these results, PLX647 treatment caused a delay in B16-IDO tumor growth and resulted in prolonged long-term survival (Fig. 2b). At day 14, the mean weight of B16-IDO tumors was three times smaller in the MDSC-depleted mice compared to mice treated with control chow (Fig. 2c). In contrast, B16-WT tumors, which exhibit significantly lower numbers of tumor-infiltrating $CD11b^+Gr1^{int}$ cells did not respond to PLX647 treatment (Fig. 2b). As PLX647 is a selective bispecific inhibitor of CSF-1R and KIT receptor tyrosine kinases (Elmore et al., 2014; Zhang et al., 2013), we performed a similar experiment with another CSF-1R inhibitor, PLX5622, which has a higher specificity for CSF-1R (Cavnar et al., 2013; Kim et al., 2014) in order to verify that the observed anti-tumor effect of PLX647 in the B16-IDO tumor model was mediated by inhibition of CSF-1R and not inhibition of KIT kinases. Therapeutic anti-tumor effects of PLX5622 and PLX647 were equivalent (Fig. 2d), further

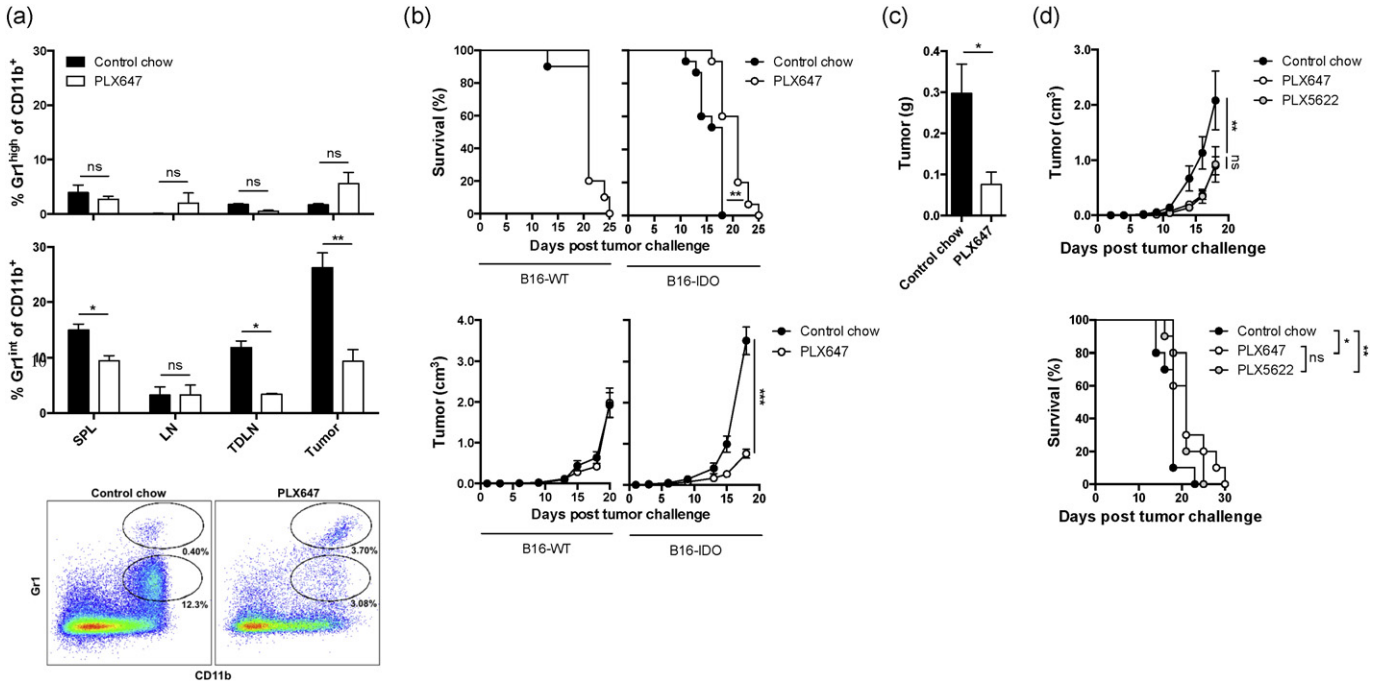

Fig. 2. CSF-1R blockade inhibits tumor growth of tumors with high MDSC infiltration by depletion of $CD11b^+Gr1^{int}$ MDSC subsets. (a) Mice were injected with B16-IDO tumor cells and treated with PLX647 or control chow. Frequencies of Gr^{high} and Gr^{int} cell subsets of total $CD11b^+$ cells in the spleen, LN, TDLN, and tumor after 2 week treatment with PLX647 or control chow, and representative flow plots of $CD11b^+Gr1^{high}$ and $CD11b^+Gr1^{int}$ cell populations of $CD45^+$ cell gated TILs after treatment with PLX647 or control chow. (b) Survival and tumor growth in mice injected with B16-IDO or B16-WT tumor cells and treated with PLX647 or control chow. (c) Tumor weights. (d) Mean tumor growth and overall survival of B16-IDO tumor-bearing mice treated with PLX647, PLX5622 or control chow. Data shown are mean ± SEM of 3 independent experiments.

suggesting that the effect is mediated through CSF-1R inhibition. These findings indicate that PLX647 specifically depletes CSF-1R-expressing MDSC subsets in the B16 tumor model and that pre-treatment presence of high levels of suppressive MDSCs is a predictive anti-tumor effect.

3.3. CSF1R Blockade Increases Anti-tumor T Cell Activity at the Tumor Site

To specifically evaluate the impact of $CD11b^+Gr1^{int}$ MDSC depletion on the tumor-specific immune responses, B16-IDO tumor-bearing mice

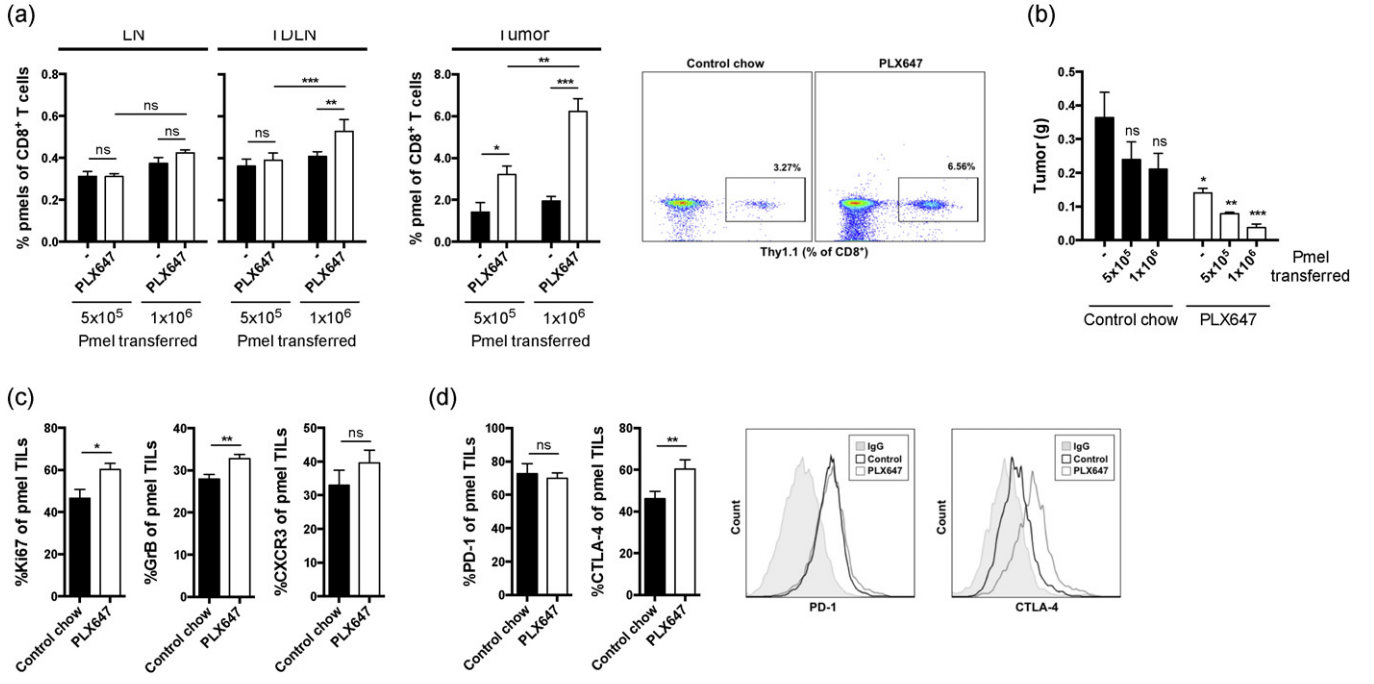

Fig. 3. CSF-1R blockade increases antigen-specific T cell activity at the tumor site. (a) Mice were injected with B16-IDO tumor cells and treated with PLX647 or control chow. Five days after tumor challenge mice adoptively received *in vitro* activated pmel $CD8^+$ T cells and were sacrificed 2 weeks after tumor challenge. Average percentage and representative dot plots of pmel cells of total $CD8^+$ T cells in LN, TDLN, and tumors in each group of mice are shown. (b) B16-IDO tumor size in mice after adoptive transfer of increasing numbers of $CD8^+$ pmel T cells and treatment with PLX647 or control chow. (c) Expression of CXCR3, Ki-67 and Granzyme B on tumor-infiltrating $CD8^+$ pmel T cells isolated from mice treated with PLX647 or control chow. (d) Percentage tumor-infiltrating $CD8^+$ pmel T cells from mice treated with PLX647 or control chow expressing PD-1 and CTLA-4 and representative flow histograms. Data are shown as mean ± SEM of 3 independent experiments.

were treated with PLX647 and adoptively transferred *in vitro* activated pmel CD8$^+$ T cells, which express transgenic T cell receptor recognizing melanoma gp100 antigen. Importantly, depletion of CD11b$^+$ Gr1^{int} cells with PLX647 resulted in significantly greater accumulation of pmel T cells at the tumor site and draining lymph nodes (Fig. 3a). This was accompanied by significant delay in tumor growth, which was most pronounced with the highest pmel dose, underscoring the active role of antigen-specific immunity mediating the anti-tumor effect (Fig. 3b). Furthermore, phenotypic characterization of pmel T cells from tumors of mice receiving PLX647 treatment demonstrated up-regulation of Granzyme B (GrB) and Ki-67, and a non-statistically-significant increase in CXCR3, over the untreated mice further indicating that the tumor-infiltrating pmel cells acquire cytotoxic phenotype (Fig. 3c).

3.4. CSF-1R blockade Potentiates the Anti-tumor Efficacy of T Cell Checkpoint Immunotherapy

As noted above, treatment with CSF-1R inhibitor alone was able to delay the tumor growth, however all of the tumors eventually grew out, resulting in only modest benefit on overall survival (Fig. 2b). Recently, it was reported that while CSF-1/CSF-1R blockade reprogrammed the tumor microenvironment to enhance effector T cell infiltration in pancreatic tumors, upregulation of T cell checkpoints was also enhanced (Zhu et al., 2014). Similarly, we observed that CTLA-4 expression on tumor-infiltrating CD8$^+$ pmel cytotoxic T lymphocytes (CTLs) was significantly upregulated by CSF-1R blockade (Fig. 3d). In addition, activated pmel CTLs in the B16-IDO tumors showed high levels of PD-1 expression (Fig. 3d), although unaffected by CSF-1R blockade (Fig. 3d). These data suggest that although CSF-1R blockade enhances T cell infiltration in B16-IDO tumors, the anti-tumor immunity may be limited *via* constitutive expression or upregulation of T cell checkpoints. Therefore, we hypothesized that CSF-1R blockade could enhance B16-IDO tumor responses to CTLA-4 and PD-1 blockade. To test this hypothesis, B16-IDO tumor-bearing mice were treated with PLX647 in combination with anti-CTLA-4 and anti-PD-1 antibodies. Anti-CTLA-4 + anti-PD-1 checkpoint alone had only very limited efficacy on the progression of B16-IDO tumors with no effect on overall survival (Fig. 4a). By contrast, the combination of PLX647 with anti-CTLA-4 + anti-PD-1 antibodies significantly reduced tumor progression and enhanced overall survival, when compared to untreated mice and mice treated with PLX647 or CTLA-4 + PD-1 antibodies alone (Fig. 4a). Analysis of T cell responses in tumors following combined therapy with PLX647 and anti-CTLA-4 + anti-PD-1 antibodies revealed a significant increase in numbers of CD45$^+$ cells and T cells in the combination therapy group (Fig. 4b). This increase in tumor infiltrating lymphocytes (TILs) was primarily due to infiltration of IFNγ$^+$CD8$^+$ and CD4$^+$ effector T cells but not Treg cells (Fig. 4c and d), leading to favorable effector to Treg ratios (Fig. 4e). The increase in number of T cells was accompanied by a decrease in CD11b$^+$ Gr1^{int} MDSCs following the combined therapeutic regimen (Fig. 4f). To determine if tumor responses in PLX647 treated mice were dependent on T cells, we conducted CD4 and CD8 T cell depletion studies. Depletion of CD4 as well as CD8 T cells significantly reduced the therapeutic effect of anti-CTLA-4 + anti-PD-1 antibodies (Fig. 4g), suggesting that CSF-1R blockade improves immunotherapy with immunomodulatory antibodies by enhancing T cell activities through depletion of CD11b$^+$ Gr1^{int} MDSCs from the tumor microenvironment. This enhancement, however, was only evident in the B16-IDO tumor model, which possesses high levels of MDSCs, but was absent in the B16-WT tumor model (data not shown).

3.5. Combination Therapy with CSF-1R and T Cell Checkpoint Blockade is Effective Against Established Colon Tumors

To determine whether the CSF-1R + T cell checkpoint blockade treatment strategy could be extended to other tumor types, we evaluated it in the CT26 colorectal carcinoma model, where expansion of MDSCs has previously been described (Dolcetti et al., 2010; Youn et al., 2008). To this end, BALB/c mice were challenged with CT26 tumor cells and treatment with PLX647 and/or anti-CTLA-4 + PD-1 was initiated 10 days after tumor inoculation when tumors exhibited a volume of approximately 50–100 mm^3. The combination of dual CSF-1R inhibition and checkpoint blockade caused a delay of tumor growth with prolonged long-term survival in a subset of mice, whereas the individual components had little to no effect on tumor growth (Fig. 4h). Thus, the therapeutic activity of the combination of CSF-1R blockade and anti-CTLA-4 + PD-1 is not restricted to the B16-IDO

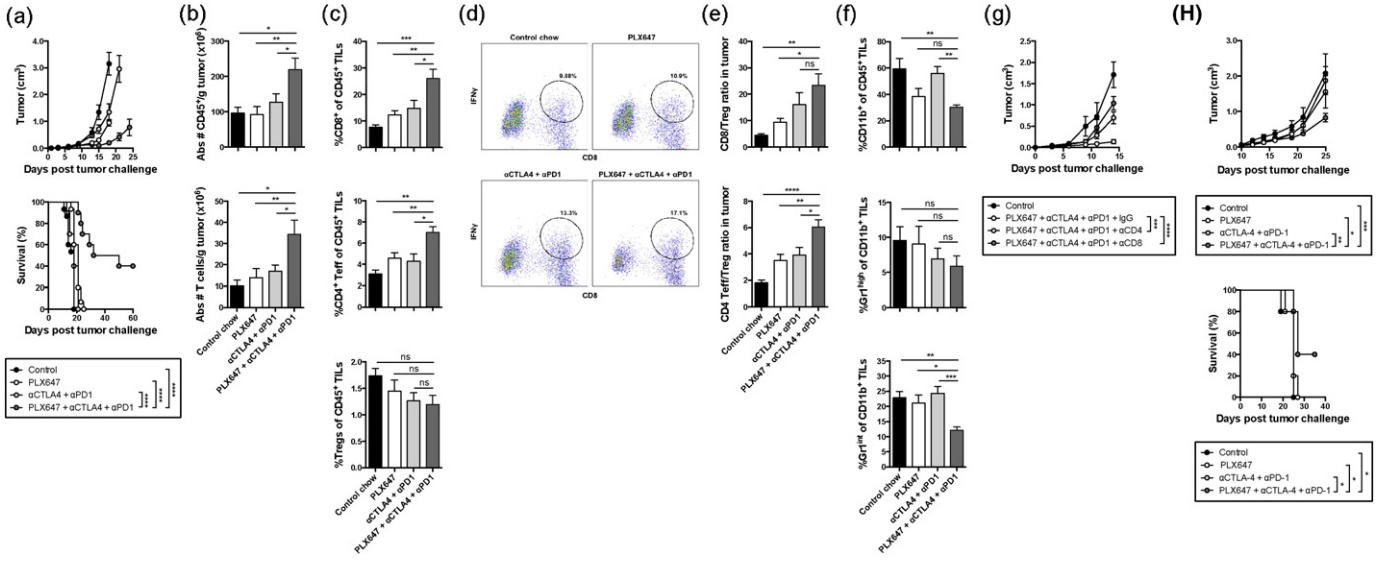

Fig. 4. CSF-1R blockade potentiates antitumor responses to checkpoint blockade. (a) Mean tumor growth and overall survival of B16-IDO tumor-bearing mice treated with PLX647 and/or aCTLA-4 + aPD-1. (b) B16-IDO tumors from mice treated with PLX647 and/or aCTLA-4 + aPD-1 were harvested 2 weeks after tumor cell inoculation and analyzed for absolute numbers of CD45$^+$ cells and T cells per gram of tumor. (c) Infiltration of CD8$^+$ T cells, CD4$^+$Foxp3$^-$ T cells and CD4$^+$Foxp3$^+$ Tregs gated on the CD45$^+$ population. (d) Representative dot plots showing IFNγ expressing CD8$^+$ T cells in response to *in vitro* stimulation with DCs. (e) Effector T cells to Treg ratios in tumors. (f) Relative percentage of total CD11b$^+$ cells and CD11b$^+$Gr1^{int} subsets of CD45$^+$ TILs. (g) Survival curves for B16-IDO tumor-bearing mice treated with PLX647 and/or aCTLA-4 + aPD-1 plus depleting antibodies for CD8 and CD4 or a corresponding dose of IgG isotype control. (h) Mean tumor growth and overall survival of CT26 tumor-bearing mice treated with PLX647 and/or aCTLA-4 + aPD-1. Data are mean ± SEM of 3 independent experiments with 5 mice/group.

tumor model. These data confirm previous findings in a pancreatic tumor model (Zhu et al., 2014).

3.6. CSF1R Blockade Potentiates the Therapeutic Effect of IDO Inhibition

The B16-IDO tumor model is characterized by high expression of IDO, which exerts immune suppression not just through recruitment of MDSCs, but also through additional mechanisms, which include direct inhibition of effector T cells and expansion and activation of Tregs (Munn and Mellor, 2007). We thus proceeded to examine whether depletion of $CD11b^{+}Gr1^{int}$ MDSCs could sensitize the tumors to IDO inhibitor-based immunotherapy. To test this hypothesis, B16-IDO tumor-bearing mice were treated with the IDO inhibitor, indoximod/D-1MT (IDOi), in combination with PLX647. While the agents were only modestly effective on their own, we observed significant tumor growth delay and an increase in overall survival with the combination therapy (Fig. 5a). This reduction in tumor growth correlated with increases in $CD8^{+}$ and $CD4^{+}$ effector T cells (Fig. 5b). Taken together, our data show that $CD11b^{+}Gr1^{int}$ MDSCs enhance tumor growth and inhibit tumor-specific immunity *in vivo*, highlighting the importance of MDSC as a therapeutic target. From a clinical perspective, these data also suggest that CSF-1R blockade might be a relevant strategy only for patients with tumors highly infiltrated with suppressive MDSCs, suggesting that clinical studies of such compounds should include pretreatment evaluation of tumor MDSCs as a potential predictive biomarker.

4. Discussion

Even though T cell checkpoint inhibitors alone have achieved impressive clinical benefit in some cancers, their application as single agents has had limited efficacy (Hamid et al., 2013; Wolchok et al., 2013). The resistance to immunotherapy is in part mediated by the immunosuppressive microenvironment in the tumor tissue, and identification of such mechanisms is highly prudent in order to develop appropriate combination strategies.

Tumor-infiltrating suppressive myeloid cells have been demonstrated to be an important component of the inhibitory tumor microenvironment and include macrophages with the M2 phenotype and MDSCs. Depending on the tumor model; different myeloid populations may be dominant. Reports have shown that some tumor models such as prostate cancer and lung carcinoma models are dominated by MDSCs and these MDSCs heavily infiltrate tumors and systemic organs such as spleen, blood, and bone marrow (Srivastava et al., 2012; Xu et al., 2013). In contrast, other tumor models have few MDSCs infiltrating the tumor or accumulating in the spleen, and are primarily dominated by macrophages (Mok et al., 2014; Pyonteck et al., 2013).

While studying the role of IDO in immune suppression, we found that tumor IDO expression induces recruitment of MDSCs to tumors in several mouse tumor models (Holmgaard et al., 2015). We thus established an IDO-expressing tumor model which allowed for studies of MDSC targeting in both MDSC-high and MDSC-low tumor types. Here we find high expression of CSF-1R on the dominant suppressive subset of MDSCs in B16-IDO tumors. Our data demonstrate that CSF-1R blockade with PLX647 decreases the quantity of MDSCs in B16-IDO tumors, leading to increased anti-tumor immunity. The blockade alone modestly enhances antitumor responses, promotes CTL infiltration, and slows tumor progression. However, the therapeutic effect of such inhibition is limited and does not induce tumor regression. Although CSF-1R blockade enhances the anti-tumor activity of myeloid cells and T cell responses, we found that its efficacy was blunted by high expression and upregulation of immune checkpoint molecules, which was

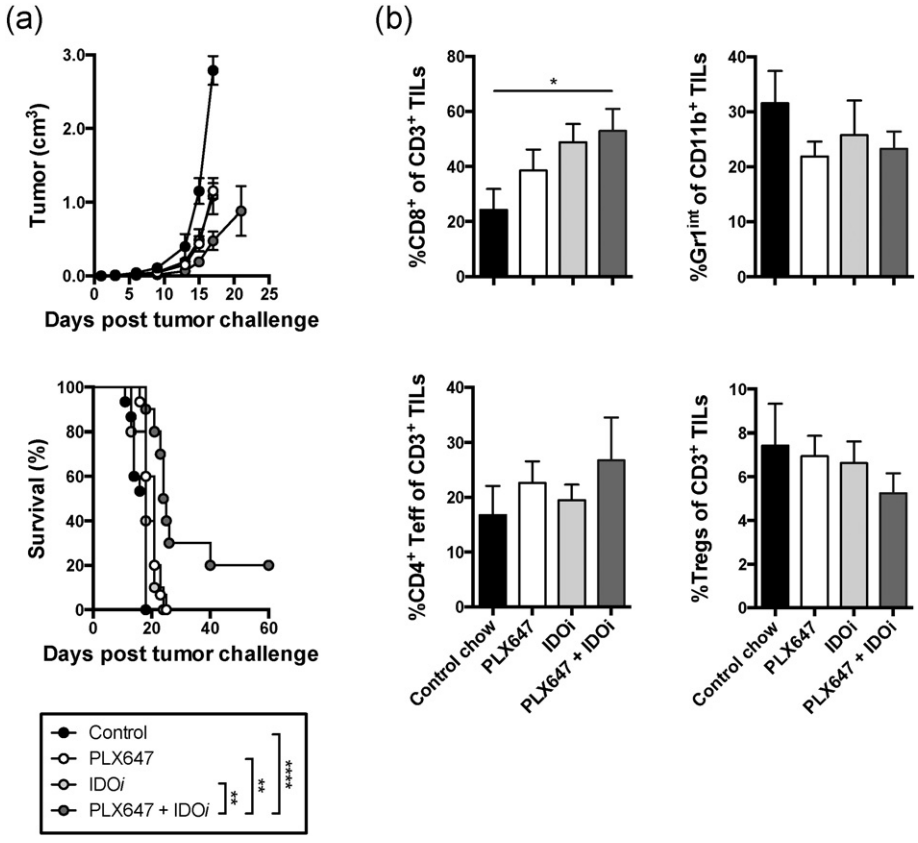

Fig. 5. CSF-1R blockade enhances responses to IDO blockade immunotherapy. (a) Mean tumor growth and overall survival of B16-IDO tumor-bearing mice treated with PLX647 and/or IDOi. (b) B16-IDO tumors from mice treated with PLX647 and/or IDOi were harvested 2 weeks after tumor cell inoculation and analyzed for infiltration of various immune cell subsets. Results for $CD4^{+}Foxp3^{+}$ Tregs, $CD8^{+}$ and $CD4^{+}$ effector T cells as percentages of total $CD3^{+}$ T cells, and $Gr1^{int}$ MDSCs as percentages of total $CD11b^{+}$ cells are shown. Data shown are mean ± SEM of 3 independent experiments with 5 mice/group (*a*) or one representative experiment of 2 (*b*).

consistent with the recent data from Zhu et al. (2014) in a pancreatic tumor model. Inhibition of CSF-1R, however, markedly improved the efficacy of checkpoint- and IDO-based immunotherapy and led to regression of established tumors. The antitumor activity of a combined therapy with CSF-1R and T cell checkpoint blockade was mediated by inhibition of the myeloid cell-mediated immunosuppressive tumor microenvironment, resulting in increased tumor infiltration with activated T cells. These studies thus suggest that the resistance to immune checkpoint blockade could be alleviated by therapeutic strategies that reprogram dominant myeloid responses to allow for effective checkpoint therapy. To this end, our group has shown that pre-treatment levels of circulating MDSCs can predict therapeutic outcomes from CTLA-4 blockade in melanoma patients (Kitano et al., 2014). The findings above were not only restricted to the B16-IDO model, but were also noted in established CT26 colon tumors.

While the IDO inhibitor therapy synergized with CSF-1R blockade in the B16-IDO tumor model, it was not as effective as the synergy between T cell checkpoint blockade and CSF-1R blockade. Tumor infiltration of MDSCs might be a result of high levels of IDO expression as recently published (Holmgaard et al., 2015), and thus, IDO inhibitors and CSF-1R blockade potentially target the same immune pathway, whereas the T cell checkpoint blockade and CSF-1R blockade therapies act on different immune components and pathways.

Several preclinical studies have suggested that inhibition of CSF-1R signaling may alter the immunologic response of tumor-infiltrating MDSCs and/or tumor-infiltrating macrophages (DeNardo et al., 2011; Mitchem et al., 2013; Mok et al., 2014; Priceman et al., 2010; Pyonteck et al., 2013; Sluijter et al., 2014; Strachan et al., 2013; Xu et al., 2013; Zhu et al., 2014). Mok et al. (2014) targeted CSF-1R signaling using PLX3397 in a murine SM1 melanoma model. PLX3397 treatment depleted more than 80% of tumor-infiltrating macrophages, leading to an increased efficacy of adoptively transferred T cell based therapies. Other studies have shown that CSF-1R blockade therapy reduced the number of MDSCs as well as macrophages in tumor and systemic organs (Priceman et al., 2010; Xu et al., 2013). Using the selective inhibitor of CSF-1R, GW2580, Priceman et al. (2010) demonstrated that CSR-1R signaling regulated recruitment of both MDSCs and M2 macrophages to lung, melanoma, and prostate tumors.

In our model, CSF-1R blockade with PLX647 mainly targeted the more abundant MDSCs instead of macrophages, suggesting that the role of CSF-1 may be tumor model-dependent. Different tumor models, genetic backgrounds, or treatments may induce different growth factors or cytokines in the tumor microenvironment. Infiltration and differentiation of myeloid cells in tumors is a complex process regulated by multiple pathways, which may lead to differential responses to CSF-1R inhibition (Li et al., 2009; Lin et al., 2008; Sawanobori et al., 2008; Wei et al., 2010). For example, while CSF-1R inhibition in pancreas melanoma and breast models resulted in reduction of macrophage numbers, in a murine glioma model Pyonteck et al. (2013) have shown that blockade of CSF-1R signaling using the small molecule inhibitor BLZ945, favorably reprograms macrophage responses without reducing their numbers. In that study, CSF-1R blockade impaired the tumor-promoting functions of M2 macrophages and led to regression of established tumors. Taken together, these results suggest that CSF-1R signaling can regulate both the number and function of tumor-infiltrating myeloid cells, but these activities may be highly dependent on the tumor type or tissue-specific factors.

Finally, by being able to study both MDSC-high and MDSC-low tumor models, we were able to evaluate the rationale for CSF-1R inhibition in both types of tumors. Perhaps not surprisingly, our results suggest that the efficacy of CSF-1R blockade is limited to tumors with high infiltration of CSF-1R expressing suppressive cells. As CSF-1R inhibitors are entering immunotherapy clinical trials, it will be important to evaluate tumor-infiltrating MDSCs and macrophages as a mechanism of resistance to immune checkpoint blockade and as a potential biomarker that could predict responses to CSF-1R inhibition.

In conclusion, we describe that blockade of CSF-1R signaling in B16-IDO tumors depletes $CD11b^{+}Gr1^{int}$ MDSCs and reprograms the tumor microenvironment to support antitumor immunity. By decreasing the presence of immunosuppressive $CD11b^{+}Gr1^{int}$ MDSCs in the tumor, PLX647 likely facilitates the intratumoral trafficking of CTLs and their antitumor functions. Furthermore, our studies suggest that MDSC inhibition alone by PLX647 is not sufficient for an efficient antitumor response in the B16-IDO tumor model. An active T cell-mediated immunotherapy is needed for an optimal antitumor effect of PLX647 and thus, the main beneficial effects of PLX647 in the B16-IDO model may be derived from the ability to improve T cell effector functions through the inhibition of intratumoral immunosuppressive MDSCs. These data suggest that CSF-1R may be an effective therapeutic target to reprogram the immunosuppressive microenvironment of human tumors strongly infiltrated with myeloid cells and provide a strong rationale for the development of new therapeutic approaches targeting CSF-1R in combination with other agents.

Conflict of Interest Statement

The authors declare that they have no competing interests.

Funding

This work was in part supported by the NIH grant R01CA56821, the NIH/NCI Cancer Center Support Grant P30CA008748, Swim Across America, Ludwig Cancer Research, and Breast Cancer Research Foundation. RBH is the recipient of postdoctoral fellowships through The Danish Cancer Society (R56-A2943-12-S2) and The Carlsberg Foundation (CF14-0224), Denmark.

Author Contributions

RBH developed the concept, designed, performed and analyzed experiments, and wrote the manuscript. DZ discussed experiments and edited and communicated regarding the manuscript. AL discussed experiments. TM and JDW supervised progress and edited the manuscript.

Acknowledgement

We would like to thank Plexxikon Inc. for providing drugs for the studies. Further, we thank Hong Zhong and Yuri Igarash (Memorial Sloan Kettering Cancer Center) for technical assistance. In addition, we thank the Flow Cytometry Facility at Memorial Sloan Kettering Cancer Center.

References

Aharinejad, S., Paulus, P., Sioud, M., Hofmann, M., Zins, K., Schafer, R., Stanley, E.R., Abraham, D., 2004. Colony-stimulating factor-1 blockade by antisense oligonucleotides and small interfering RNAs suppresses growth of human mammary tumor xenografts in mice. Cancer Res. 64, 5378–5384.

Caescu, C.I., Guo, X., Tesfa, L., Bhagat, T.D., Verma, A., Zheng, D., Stanley, E.R., 2015. Colony stimulating factor-1 receptor signaling networks inhibit mouse macrophage inflammatory responses by induction of microRNA-21. Blood 125, e1–13.

Cavnar, M.J., Zeng, S., Kim, T.S., Sorenson, E.C., Ocuin, L.M., Balachandran, V.P., Seifert, A.M., Greer, J.B., Popow, R., Crawley, M.H., Cohen, N.A., Green, B.L., Rossi, F., Besmer, P., Antonescu, C.R., DeMatteo, R.P., 2013. KIT oncogene inhibition drives intratumoral macrophage M2 polarization. J. Exp. Med. 210, 2873–2886.

Coniglio, S.J., Eugenin, E., Dobrenis, K., Stanley, E.R., West, B.L., Symons, M.H., Segall, J.E., 2012. Microglial stimulation of glioblastoma invasion involves epidermal growth factor receptor (EGFR) and colony stimulating factor 1 receptor (CSF-1R) signaling. Mol. Med. 18, 519–527.

Curran, M.A., Allison, J.P., 2009. Tumor vaccines expressing flt3 ligand synergize with ctla-4 blockade to reject preimplanted tumors. Cancer Res. 69, 7747–7755.

Dai, X.M., Ryan, G.R., Hapel, A.J., Dominguez, M.G., Russell, R.G., Kapp, S., Sylvestre, V., Stanley, E.R., 2002. Targeted disruption of the mouse colony-stimulating factor 1 receptor gene results in osteopetrosis, mononuclear phagocyte deficiency, increased primitive progenitor cell frequencies, and reproductive defects. Blood 99, 111–120.

DeNardo, D.G., Brennan, D.J., Rexhepaj, E., Ruffell, B., Shiao, S.L., Madden, S.F., Gallagher, W.M., Wadhwani, N., Keil, S.D., Junaid, S.A., Rugo, H.S., Hwang, E.S., Jirstrom, K.,

West, B.L., Coussens, L.M., 2011. Leukocyte complexity predicts breast cancer survival and functionally regulates response to chemotherapy. Cancer Discov. 1, 54–67.
Diatta, A., Piver, E., Collin, C., Vaudin, P., Pages, J.C., 2005. Semliki Forest virus-derived virus-like particles: characterization of their production and transduction pathways. J. Gen. Virol. 86, 3129–3136.
Diaz-Montero, C.M., Salem, M.L., Nishimura, M.I., Garrett-Mayer, E., Cole, D.J., Montero, A.J., 2009. Increased circulating myeloid-derived suppressor cells correlate with clinical cancer stage, metastatic tumor burden, and doxorubicin-cyclophosphamide chemotherapy. Cancer Immunol. Immunother. 58, 49–59.
Dolcetti, L., Peranzoni, E., Ugel, S., Marigo, I., Fernandez Gomez, A., Mesa, C., Geilich, M., Winkels, G., Traggiai, E., Casati, A., Grassi, F., Bronte, V., 2010. Hierarchy of immunosuppressive strength among myeloid-derived suppressor cell subsets is determined by GM-CSF. Eur. J. Immunol. 40, 22–35.
Elmore, M.R., Najafi, A.R., Koike, M.A., Dagher, N.N., Spangenberg, E.E., Rice, R.A., Kitazawa, M., Matusow, B., Nguyen, H., West, B.L., Green, K.N., 2014. Colony-stimulating factor 1 receptor signaling is necessary for microglia viability, unmasking a microglia progenitor cell in the adult brain. Neuron 82, 380–397.
Gabrilovich, D.I., Nagaraj, S., 2009. Myeloid-derived suppressor cells as regulators of the immune system. Nat. Rev. Immunol. 9, 162–174.
Gunturu, K.S., Rossi, G.R., Saif, M.W., 2013. Immunotherapy updates in pancreatic cancer: are we there yet? Ther.Adv.Med.Oncol. 5, 81–89.
Hamid, O., Robert, C., Daud, A., Hodi, F.S., Hwu, W.J., Kefford, R., Wolchok, J.D., Hersey, P., Joseph, R.W., Weber, J.S., Dronca, R., Gangadhar, T.C., Patnaik, A., Zarour, H., Joshua, A.M., Gergich, K., Elassaiss-Schaap, J., Algazi, A., Mateus, C., Boasberg, P., Tumeh, P.C., Chmielowski, B., Ebbinghaus, S.W., Li, X.N., Kang, S.P., Ribas, A., 2013. Safety and tumor responses with lambrolizumab (anti-PD-1) in melanoma. N. Engl. J. Med. 369, 134–144.
Hodi, F.S., Mihm, M.C., Soiffer, R.J., Haluska, F.G., Butler, M., Seiden, M.V., Davis, T., Henry-Spires, R., MacRae, S., Willman, A., Padera, R., Jaklitsch, M.T., Shankar, S., Chen, T.C., Korman, A., Allison, J.P., Dranoff, G., 2003. Biologic activity of cytotoxic T lymphocyte-associated antigen 4 antibody blockade in previously vaccinated metastatic melanoma and ovarian carcinoma patients. Proc. Natl. Acad. Sci. U. S. A. 100, 4712–4717.
Hodi, F.S., O'Day, S.J., McDermott, D.F., Weber, R.W., Sosman, J.A., Haanen, J.B., Gonzalez, R., Robert, C., Schadendorf, D., Hassel, J.C., Akerley, W., van den Eertwegh, A.J., Lutzky, J., Lorigan, P., Vaubel, J.M., Linette, G.P., Hogg, D., Ottensmeier, C.H., Lebbe, C., Peschel, C., Quirt, I., Clark, J.I., Wolchok, J.D., Weber, J.S., Tian, J., Yellin, M.J., Nichol, G.M., Hoos, A., Urba, W.J., 2010. Improved survival with ipilimumab in patients with metastatic melanoma. N. Engl. J. Med. 363, 711–723.
Holmgaard, R.B., Zamarin, D., Munn, D.H., Wolchok, J.D., Allison, J.P., 2013. Indoleamine 2,3-dioxygenase is a critical resistance mechanism in antitumor T cell immunotherapy targeting CTLA-4. J. Exp. Med. 210, 1389–1402.
Holmgaard, R.B., Zamarin, D., Li, Y., Gasmi, B., Munn, D.H., Allison, J.P., Merghoub, T., Wolchok, J.D., 2015. Tumor-expressed IDO Recruits and activates MDSCs in a Treg-dependent manner. Cell Rep. 13, 412–424.
Kerkar, S.P., Restifo, N.P., 2012. Cellular constituents of immune escape within the tumor microenvironment. Cancer Res. 72, 3125–3130.
Kim, T.S., Cavnar, M.J., Cohen, N.A., Sorenson, E.C., Greer, J.B., Seifert, A.M., Crawley, M.H., Green, B.L., Popow, R., Pillarsetty, N., Veach, D.R., Ku, A.T., Rossi, F., Besmer, P., Antonescu, C.R., Zeng, S., Dematteo, R.P., 2014. Increased KIT inhibition enhances therapeutic efficacy in gastrointestinal stromal tumor. Clin. Cancer Res. 20, 2350–2362.
Kitano, S., Postow, M.A., Ziegler, C.G., Kuk, D., Panageas, K.S., Cortez, C., Rasalan, T., Adamow, M., Yuan, J., Wong, P., Altan-Bonnet, G., Wolchok, J.D., Lesokhin, A.M., 2014. Computational algorithm-driven evaluation of monocytic myeloid-derived suppressor cell frequency for prediction of clinical outcomes. CancerImmunol.Res. 2, 812–821.
Le, D.T., Lutz, E., Uram, J.N., Sugar, E.A., Onners, B., Solt, S., Zheng, L., Diaz Jr., L.A., Donehower, R.C., Jaffee, E.M., Laheru, D.A., 2013. Evaluation of ipilimumab in combination with allogeneic pancreatic tumor cells transfected with a GM-CSF gene in previously treated pancreatic cancer. J. Immunother. 36, 382–389.
Li, J., Chen, K., Zhu, L., Pollard, J.W., 2006. Conditional deletion of the colony stimulating factor-1 receptor (c-fms proto-oncogene) in mice. Genesis 44, 328–335.
Li, X., Loberg, R., Liao, J., Ying, C., Snyder, L.A., Pienta, K.J., McCauley, L.K., 2009. A destructive cascade mediated by CCL2 facilitates prostate cancer growth in bone. Cancer Res. 69, 1685–1692.
Lin, H., Lee, E., Hestir, K., Leo, C., Huang, M., Bosch, E., Halenbeck, R., Wu, G., Zhou, A., Behrens, D., Hollenbaugh, D., Linnemann, T., Qin, M., Wong, J., Chu, K., Doberstein, S.K., Williams, L.T., 2008. Discovery of a cytokine and its receptor by functional screening of the extracellular proteome. Science 320, 807–811.
Lutz, E., Yeo, C.J., Lillemoe, K.D., Biedrzycki, B., Kobrin, B., Herman, J., Sugar, E., Piantadosi, S., Cameron, J.L., Solt, S., Onners, B., Tartakovsky, I., Choi, M., Sharma, R., Illei, P.B., Hruban, R.H., Abrams, R.A., Le, D., Jaffee, E., Laheru, D., 2011. A lethally irradiated allogeneic granulocyte-macrophage colony stimulating factor-secreting tumor vaccine for pancreatic adenocarcinoma. A phase II trial of safety, efficacy, and immune activation. Ann. Surg. 253, 328–335.
Manthey, C.L., Johnson, D.L., Illig, C.R., Tuman, R.W., Zhou, Z., Baker, J.F., Chaikin, M.A., Donatelli, R.R., Franks, C.F., Zeng, L., Crysler, C., Chen, Y., Yurkow, E.J., Boczon, L., Meegalla, S.K., Wilson, K.J., Wall, M.J., Chen, J., Ballentine, S.K., Ott, H., Baumann, C., Lawrence, D., Tomczuk, B.E., Molloy, C.J., 2009. JNJ-28312141, a novel orally active colony-stimulating factor-1 receptor/FMS-related receptor tyrosine kinase-3 receptor tyrosine kinase inhibitor with potential utility in solid tumors, bone metastases, and acute myeloid leukemia. Mol. Cancer Ther. 8, 3151–3161.
Mitchem, J.B., Brennan, D.J., Knolhoff, B.L., Belt, B.A., Zhu, Y., Sanford, D.E., Belaygorod, L., Carpenter, D., Collins, L., Piwnica-Worms, D., Hewitt, S., Udupi, G.M., Gallagher, W.M., Wegner, C., West, B.L., Wang-Gillam, A., Goedegebuure, P., Linehan, D.C., DeNardo, D.G., 2013. Targeting tumor-infiltrating macrophages decreases tumor-initiating cells, relieves immunosuppression, and improves chemotherapeutic responses. Cancer Res. 73, 1128–1141.
Mok, S., Koya, R.C., Tsui, C., Xu, J., Robert, L., Wu, L., Graeber, T.G., West, B.L., Bollag, G., Ribas, A., 2014. Inhibition of CSF-1 receptor improves the antitumor efficacy of adoptive cell transfer immunotherapy. Cancer Res. 74, 153–161.
Munn, D.H., Mellor, A.L., 2007. Indoleamine 2,3-dioxygenase and tumor-induced tolerance. J. Clin. Invest. 117, 1147–1154.
Overwijk, W.W., Theoret, M.R., Finkelstein, S.E., Surman, D.R., de Jong, L.A., Vyth-Dreese, F.A., Dellemijn, T.A., Antony, P.A., Spiess, P.J., Palmer, D.C., Heimann, D.M., Klebanoff, C.A., Yu, Z., Hwang, L.N., Feigenbaum, L., Kruisbeek, A.M., Rosenberg, S.A., Restifo, N.P., 2003. Tumor regression and autoimmunity after reversal of a functionally tolerant state of self-reactive CD8 + T cells. J. Exp. Med. 198, 569–580.
Patel, S., Player, M.R., 2009. Colony-stimulating factor-1 receptor inhibitors for the treatment of cancer and inflammatory disease. Curr. Top. Med. Chem. 9, 599–610.
Phan, G.Q., Yang, J.C., Sherry, R.M., Hwu, P., Topalian, S.L., Schwartzentruber, D.J., Restifo, N.P., Haworth, L.R., Seipp, C.A., Freezer, L.J., Morton, K.E., Mavroukakis, S.A., Duray, P.H., Steinberg, S.M., Allison, J.P., Davis, T.A., Rosenberg, S.A., 2003. Cancer regression and autoimmunity induced by cytotoxic T lymphocyte-associated antigen 4 blockade in patients with metastatic melanoma. Proc. Natl. Acad. Sci. U. S. A. 100, 8372–8377.
Priceman, S.J., Sung, J.L., Shaposhnik, Z., Burton, J.B., Torres-Collado, A.X., Moughon, D.L., Johnson, M., Lusis, A.J., Cohen, D.A., Iruela-Arispe, M.L., Wu, L., 2010. Targeting distinct tumor-infiltrating myeloid cells by inhibiting CSF-1 receptor: combating tumor evasion of antiangiogenic therapy. Blood 115, 1461–1471.
Pyonteck, S.M., Akkari, L., Schuhmacher, A.J., Bowman, R.L., Sevenich, L., Quail, D.F., Olson, O.C., Quick, M.L., Huse, J.T., Teijeiro, V., Setty, M., Leslie, C.S., Oei, Y., Pedraza, A., Zhang, J., Brennan, C.W., Sutton, J.C., Holland, E.C., Daniel, D., Joyce, J.A., 2013. CSF-1R inhibition alters macrophage polarization and blocks glioma progression. Nat. Med. 19, 1264–1272.
Ribas, A., Comin-Anduix, B., Economou, J.S., Donahue, T.R., de la Rocha, P., Morris, L.F., Jalil, J., Dissette, V.B., Shintaku, I.P., Glaspy, J.A., Gomez-Navarro, J., Cochran, A.J., 2009. Intratumoral immune cell infiltrates, FoxP3, and indoleamine 2,3-dioxygenase in patients with melanoma undergoing CTLA4 blockade. Clin. Cancer Res. 15, 390–399.
Richardsen, E., Uglehus, R.D., Johnsen, S.H., Busund, L.T., 2015. Macrophage-colony stimulating factor (CSF1) predicts breast cancer progression and mortality. Anticancer Res. 35, 865–874.
Robert, C., Thomas, L., Bondarenko, I., O'Day, S., D J M, Garbe, C., Lebbe, C., Baurain, J.F., Testori, A., Grob, J.J., Davidson, N., Richards, J., Maio, M., Hauschild, A., Miller Jr., W.H., Gascon, P., Lotem, M., Harmankaya, K., Ibrahim, R., Francis, S., Chen, T.T., Humphrey, R., Hoos, A., Wolchok, J.D., 2011. Ipilimumab plus dacarbazine for previously untreated metastatic melanoma. N. Engl. J. Med. 364, 2517–2526.
Royal, R.E., Levy, C., Turner, K., Mathur, A., Hughes, M., Kammula, U.S., Sherry, R.M., Topalian, S.L., Yang, J.C., Lowy, I., Rosenberg, S.A., 2010. Phase 2 trial of single agent Ipilimumab (anti-CTLA-4) for locally advanced or metastatic pancreatic adenocarcinoma. J. Immunother. 33, 828–833.
Sawanobori, Y., Ueha, S., Kurachi, M., Shimaoka, T., Talmadge, J.E., Abe, J., Shono, Y., Kitabatake, M., Kakimi, K., Mukaida, N., Matsushima, K., 2008. Chemokine-mediated rapid turnover of myeloid-derived suppressor cells in tumor-bearing mice. Blood 111, 5457–5466.
Sluijter, M., van der Sluis, T.C., van der Velden, P.A., Versluis, M., West, B.L., van der Burg, S.H., van Hall, T., 2014. Inhibition of CSF-1R supports T-cell mediated melanoma therapy. PLoS One 9, e104230.
Srivastava, M.K., Zhu, L., Harris-White, M., Kar, U.K., Huang, M., Johnson, M.F., Lee, J.M., Elashoff, D., Strieter, R., Dubinett, S., Sharma, S., 2012. Myeloid suppressor cell depletion augments antitumor activity in lung cancer. PLoS One 7, e40677.
Strachan, D.C., Ruffell, B., Oei, Y., Bissell, M.J., Coussens, L.M., Pryer, N., Daniel, D., 2013. CSF1R inhibition delays cervical and mammary tumor growth in murine models by attenuating the turnover of tumor-associated macrophages and enhancing infiltration by CD8 T cells. Oncoimmunology 2, e26968.
Tarhini, A.A., Butterfield, L.H., Shuai, Y., Gooding, W.E., Kalinski, P., Kirkwood, J.M., 2012. Differing patterns of circulating regulatory T cells and myeloid-derived suppressor cells in metastatic melanoma patients receiving anti-CTLA4 antibody and interferon-alpha or TLR-9 agonist and GM-CSF with peptide vaccination. J. Immunother. 35, 702–710.
Wei, S., Nandi, S., Chitu, V., Yeung, Y.G., Yu, W., Huang, M., Williams, L.T., Lin, H., Stanley, E.R., 2010. Functional overlap but differential expression of CSF-1 and IL-34 in their CSF-1 receptor-mediated regulation of myeloid cells. J. Leukoc. Biol. 88, 495–505.
Wolchok, J.D., Kluger, H., Callahan, M.K., Postow, M.A., Rizvi, N.A., Lesokhin, A.M., Segal, N.H., Ariyan, C.E., Gordon, R.A., Reed, K., Burke, M.M., Caldwell, A., Kronenberg, S.A., Agunwamba, B.U., Zhang, X., Lowy, I., Inzunza, H.D., Feely, W., Horak, C.E., Hong, Q., Korman, A.J., Wigginton, J.M., Gupta, A., Sznol, M., 2013. Nivolumab plus ipilimumab in advanced melanoma. N. Engl. J. Med. 369, 122–133.
Xu, J., Escamilla, J., Mok, S., David, J., Priceman, S., West, B., Bollag, G., McBride, W., Wu, L., 2013. CSF1R signaling blockade stanches tumor-infiltrating myeloid cells and improves the efficacy of radiotherapy in prostate Cancer. Cancer Res. 73, 2782–2794.
Youn, J.I., Nagaraj, S., Collazo, M., Gabrilovich, D.I., 2008. Subsets of myeloid-derived suppressor cells in tumor-bearing mice. J. Immunol. 181, 5791–5802.
Zhang, C., Ibrahim, P.N., Zhang, J., Burton, E.A., Habets, G., Zhang, Y., Powell, B., West, B.L., Matusow, B., Tsang, G., Shellooe, R., Carias, H., Nguyen, H., Marimuthu, A., Zhang, K.Y., Oh, A., Bremer, R., Hurt, C.R., Artis, D.R., Wu, G., Nespi, M., Spevak, W., Lin, P., Nolop, K., Hirth, P., Tesch, G.H., Bollag, G., 2013. Design and pharmacology of a highly specific dual FMS and KIT kinase inhibitor. Proc. Natl. Acad. Sci. U. S. A. 110, 5689–5694.
Zhu, Y., Knolhoff, B.L., Meyer, M.A., Nywening, T.M., West, B.L., Luo, J., Wang-Gillam, A., Goedegebuure, S.P., Linehan, D.C., DeNardo, D.G., 2014. CSF1/CSF1R blockade reprograms tumor-infiltrating macrophages and improves response to T-cell checkpoint immunotherapy in pancreatic cancer models. Cancer Res. 74, 5057–5069.